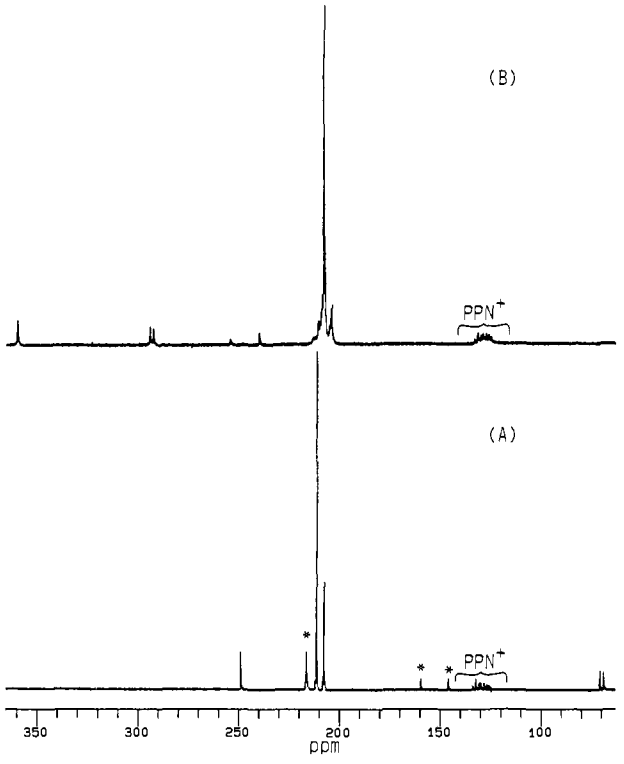

Figure 2. The ^{13}C NMR spectra (proton coupled) of $Fe_3(*CO)_9(H*C*C(O)CH_2CH_3)$ (A) and the same sample after warming to room temperature (B). The spectra were recorded at −90 °C as CD_2Cl_2 solutions. The peaks marked with an asterisk are due to unreacted $[Fe_3(*CO)_9(*C*COCH_2CH_3)]^-$.

Reactions of **3a** and **3b** with methyl triflate were also investigated. Both of these reactions were very slow (>3 days with a fivefold excess of methyl triflate) and yielded complex mixtures of products. Mass spectral analysis of the cluster products from the reaction with **3b** indicated some substitution of methyl groups for ethyl groups on the alkyne ligands. These reactions were not pursued.

Reactivity of Anionic Ketenylidene Clusters. As evidenced by previous work[5] and this study, the cluster anion in **1** can react with electrophiles at either the α-carbon or oxygen atoms of the ketenylidene moiety. The reasons for the site preference are still not clear. The acetylide clusters that are formed by attack at the oxygen atom do not appear to be metastable products since conversion to alkylidyne systems is not observed. No change was detected when a dichloromethane solution of **2b** and **3b** was left standing for 1 day or when a THF solution of **3a** was refluxed for 4 h. Steric effects would appear to play a role, as protonation of **1** occurs exclusively at the α-carbon atom[5] and larger electrophiles are observed to only react at the oxygen atom. However, other factors must also contribute to the complex reactivity since the reaction of **1** with methyl iodide leads to a single product whereas methyl triflate yields a mixture of two products.

In summary, the anionic ketenylidene cluster $[Fe_3(CO)_9(CCO)]^{2-}$ reacts with bulkier carbocation reagents to produce acetylide clusters of the general formula $[Fe_3(CO)_9(CCOR)]^-$. This result contrasts with the formation of an alkylidyne $[Fe_3(CO)_{10}(CR)]^-$ upon reaction with CH_3I.[5] This difference in reactivity is attributed to easier access of the ketenylidene oxygen to bulky electrophiles. The acetylide clusters are very reactive and are protonated to yield unstable alkyne clusters. When the ethyl derivative is warmed, clean scission of the carbon–carbon bond is observed to yield two alkylidyne fragments. This unusual instability may be due to a weakening of the carbon–carbon bond by the orientation of the alkyne ligand and the presence of an electron-withdrawing group bound to the alkyne carbon atom.

Tables of crystal data, positional parameters, bond lengths, bond angles, anisotropic thermal parameters, and observed and calculated structure factors for $[PPN][Fe_3(CO)_9(CCOC(O)CH_3)]$ are available as submitted in ref 9.

Acknowledgment. This research was supported by the National Science Foundation through Grants CHE-8204401 and CHE-8506011.

Alkylation Reactions of the CCO Ligand in Triruthenium Carbonyl Clusters. Synthesis and X-ray Crystal Structure of $Ru_3(CO)_9(\mu_3\text{-}CO)(\mu_3\text{-}C{=}C(OCH_3)CH_3)$

M. J. Sailor, C. P. Brock, and D. F. Shriver*

Contribution from the Department of Chemistry, Northwestern University, Evanston, Illinois 60208. *Received February 24, 1987*

Abstract: Alkylation reactions of the series of ruthenium ketenylidenes $[Ru_3(CO)_6(\mu\text{-}CO)_3(\mu_3\text{-}CCO)]^{2-}$ (**1**), $[HRu_3(CO)_9(\mu_3\text{-}CCO)]^-$ (**2**), and $H_2Ru_3(CO)_9(\mu_3\text{-}CCO)$ (**3**) were studied. The dinegative cluster **1** is attacked by the electrophile CH_3I to produce the acetyl cluster $[Ru_3(CO)_{10}(\mu_3\text{-}CC(O)CH_3)]^-$ (**4**). ^{13}C-labeling experiments show that the acyl CO in **4** is derived from a metal-bound carbonyl ligand on **1**, instead of from the CO of the CCO ligand. An alkylation mechanism consistent with the observations is proposed. The product of the reaction of **1** with CH_3I reacts further with the strong alkylating reagent $CH_3OSO_2CF_3$ to produce the vinylidene cluster $Ru_3(CO)_9(\mu_3\text{-}CO)(\mu_3\text{-}C{=}C(OCH_3)CH_3)$ (**5**) which has been characterized by a single-crystal X-ray structure determination. Compound **5** readily reacts with H_2 with concomitant CO loss to produce $H_2Ru_3(CO)_9(\mu_3\text{-}C{=}C(OCH_3)CH_3)$ (**6**). In contrast to the nucleophilicity of dianion **1**, the mononegative and neutral clusters $[HRu_3(CO)_9(\mu_3\text{-}CCO)]^-$ (**2**) and $H_2Ru_3(CO)_9(\mu_3\text{-}CCO)$ (**3**) are electrophilic, as demonstrated by their reaction with the nucleophile $LiCH_3$. In either case, attack by $LiCH_3$ occurs at the β-carbon of the CCO ligand. Extended Hückel molecular orbital calculations suggest that the observed reactions of **2** and **3** with nucleophiles are orbital-controlled reactions. The ^{13}C NMR data reported for the compounds include carbon–carbon coupling constants for the capping ligands. Crystals of **5** are monoclinic of space group $P2_1/n$ with a = 8.3993 (17) Å, b = 15.9259 (16) Å, c = 14.1140 (13) Å, β = 90.95 (1)°, V = 1887.73 Å,^{3} and d_{calcd} = 2.296 g/cm^3 for Z = 4. Refinement of 254 variables on 4067 reflections with $I > 3\sigma(I)$ converged at R = 0.025 and R_w = 0.052.

In the course of studies on metal cluster ketenylidenes, we discovered that the doubly negative ruthenium ketenylidene $[Ru_3(CO)_9(\mu_3\text{-}CCO)]^{2-}$ (**1**) protonates sequentially on the metal framework to yield the mononegative ketenylidene $[HRu_3$-

0002-7863/87/1509-6015$01.50/0

Table I. ^{13}C NMR Data of CCO- and CCO-Derived Ligands[a]

compound	α-carbon	β-carbon	$^1J_{CC}$, Hz
$[PPN]_2[Ru_3(CO)_9(\mu_3\text{-}CCO)]$ (1)	−28.3	159.1	97
$[PPN][HRu_3(CO)_9(\mu_3\text{-}CCO)]$ (2)[b]	50.1	165.1	78
$H_2Ru_3(CO)_9(\mu_3\text{-}CCO)$ (3)	38.7	158.8	78
$[PPN][Ru_3(CO)_{10}(\mu_3\text{-}CC(O)CH_3]$ (4)	191.8	212.7	44
$Ru_3(CO)_{10}(\mu_3\text{-}CC(OCH_3)CH_3)$ (5)	168.7	192.8	55
$H_2Ru_3(CO)_9(\mu_3\text{-}CC(OCH_3)CH_3)$ (6)	214.2	149.8	50
$H_2Ru_3(CO)_9(\mu_3,\eta^2\text{-}CHC(O)CH_3)$ (7)	74.3	239.5	43

[a] Chemical shifts in parts per million. All spectra run at −90 °C in CD_2Cl_2 and referenced with respect to $^{13}CD_2Cl_2$ at 53.8 ppm unless otherwise noted. [b] Spectrum run in THF-d_8, referenced with respect to the solvent.

$(CO)_9(\mu_3\text{-}CCO)]^-$ (2) and the previously synthesized neutral ketenylidene $H_2Ru_3(CO)_9(\mu_3\text{-}CCO)$ (3)[1] (eq 1). Such behavior

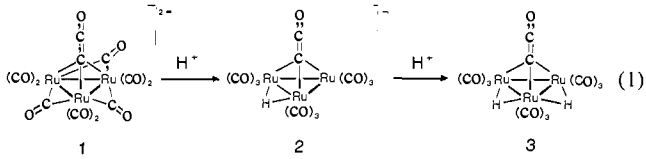

(1)

contrasts with the chemistry of the isoelectronic iron analogue $[Fe_3(CO)_9(\mu_3\text{-}CCO)]^{2-}$, which undergoes cleavage of the C=C bond of the CCO ligand upon protonation[2] (eq 2). The existence

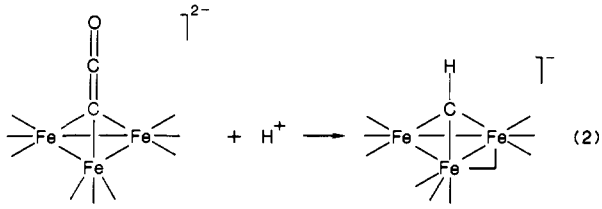
(2)

of the series of ruthenium ketenylidenes **1–3** presented the opportunity to investigate the reactivity of the CCO ligand as a function of the charge on the metal cluster. Previous work established that the dianionic ketenylidene $[Fe_3(CO)_9(\mu_3\text{-}CCO)]^{2-}$ reacts with electrophiles[2] whereas the cationic ketenylidenes $[H_3M_3(CO)_9(\mu_3\text{-}CCO)]^+$ (M = Ru, Os) or $[Co_3(CO)_9(\mu_3\text{-}CCO)]^+$ react with nucleophiles.[3-5] In the present report we describe the reactivity of the ruthenium ketenylidenes **1–3** with carbon-based electrophiles and nucleophiles. We find that the neutral cluster $H_2Ru_3(CO)_9(\mu_3\text{-}CCO)$ (3) and the monoanion $[HRu_3(CO)_9(\mu_3\text{-}CCO)]^-$ (2) are reactive toward nucleophiles while the dianion $[Ru_3(CO)_9(\mu_3\text{-}CCO)]^{2-}$ (1) reacts readily with electrophiles. Although these reactivity trends parallel the previous observations cited above, the products formed in the ruthenium system are profoundly different. Some of this work has been reported in a preliminary communication.[1]

Experimental Section

General Comments. All manipulations were carried out under a dry dinitrogen atmosphere by using standard Schlenk and syringe techniques[6] or in a Vacuum Atmospheres drybox, unless otherwise noted. Solvents were distilled from the appropriate drying agents before use.[7] The reagent $LiCH_3$ (low halide) was obtained as a 1.2 M solution in ether from Aldrich Chemicals, Inc., and used without further purification. The compound $Ru_3(CO)_{12}$ was prepared by the literature method.[8] Bis(triphenylphosphine)nitrogen(1+) chloride (PPN^+Cl^-) was purchased from Aldrich Chemicals, Inc., or Alfa Products and dried in an oven at 110 °C for 24 h prior to use. Acetyl chloride was distilled from PCl_5 and redistilled from dry quinoline before use.

Infrared spectra were recorded on a Perkin-Elmer 283 spectrometer. A JEOL FX-270 or a Varian XL-400 spectrometer was used to record the ^1H and ^{13}C spectra. The reference for ^1H and ^{13}C spectra was external Me_4Si. The ^{13}C spectra reported here are proton-decoupled unless otherwise stated. Mass spectra were obtained on a Hewlett-Packard 5985A operating in 70-eV electron-impact mode. Elemental analyses were performed by Galbraith Laboratories.

Preparation of $[PPN]_2[Ru_3(CO)_6(\mu\text{-}CO)_3(\mu_3\text{-}CCO)]$ (1). An 800-mg (1.3-mmol) sample of $Ru_3(CO)_{12}$ and 1.6 g (2.8 mmol) of [PPN]Cl were placed in a 300-mL Schlenk flask, and 20 mL of THF was added by cannula. The mixture was stirred for 1 h, during which time all the solid $Ru_3(CO)_{12}$ went into solution and the solution became dark red-brown. Twenty milliliters of a reducing solution prepared by stirring 1 g of benzophenone, 0.3 g of sodium, and 30 mL of THF vigorously for 45 min was added dropwise to the dark red-brown chloro adduct.[9] Methanol (1 mL) was then added with stirring, followed by 40 mL of diethyl ether. The resulting microcrystalline precipitate was filtered, washed with two 10-mL aliquots of methanol followed by two 10-mL aliquots of ether, and dried in vacuo. This produced crude $[PPN]_2[Ru_3(CO)_{11}]$ which was used in the next step without further purification. The IR spectrum of the resulting red-brown crystalline product matches that reported previously for this compound.[12] Anal. Calcd (Found) for $C_{83}H_{60}N_2O_{11}P_4Ru_3$: C, 59.04 (58.04); H, 3.58 (3.67); N, 1.67 (1.56); Ru, 17.96 (16.63). The solid $[PPN]_2[Ru_3(CO)_{11}]$ was transferred to a 100-mL Schlenk flask, and 25 mL of THF was added. The slurry was stirred rapidly as 0.12 mL (1.7 mmol) of CH_3COCl was added dropwise. After 20 min of stirring the THF solution was dark red-brown and a small amount of white solid was present. The benzophenone ketyl reducing solution (10 mL) was added to the slurry with stirring. Forty milliliters of diethyl ether was added producing a light brown precipitate, which was collected by filtration, washed with two 10-mL aliquots of ether, and dried in vacuo. The crude $[PPN]_2[Ru_3(CO)_9(CCO)]$ was recrystallized from dichloromethane/ether and then from acetone/ether, yielding 0.93 g (44% based on starting $Ru_3(CO)_{12}$) of orange crystals: IR (ν_{CO}, CH_2Cl_2) 2022 (m), 1980 (s), 1951 (vs), 1898 (m), 1800 (vw), 1750 (m) cm^{-1}. Anal. Calcd (Found) for $C_{83}H_{60}N_2O_{10}P_4Ru_3$: C, 59.61 (59.47); H, 3.62 (3.67); N, 1.68 (1.64); Ru, 18.13 (19.54).

^{13}C Enrichment of 1 (at All Carbons). The procedure was similar to the one above except that before the THF slurry of $Ru_3(CO)_{12}$ and [PPN]Cl was stirred, the solvent was frozen in liquid nitrogen, the flask was evacuated, and 200 torr of 99% ^{13}CO was added at ca. 150 K (free volume in the flask ca. 0.3 L). The flask was thawed and stirred for an hour. This led to ca. 30% ^{13}C enrichment. The reduction to $[Ru_3(CO)_{11}]^{2-}$, acylation to $[Ru_3(CO)_{10}(\mu\text{-}COC(O)CH_3]^-$, and reduction to $[Ru_3(CO)_9((\mu_3\text{-}CCO))]^{2-}$ was carried out as described above, and the yield was comparable. ^{13}C NMR (−90 °C, CD_2Cl_2): δ 273.3 (3μ-CO), 204.0, 202.3 (3:3) (terminal CO's), 159.1 (*CCO*, $^1J_{CC}$ = 96 Hz), −28.3 (*CCO*, $^1J_{CC}$ = 96 Hz).

Selective ^{13}C Enrichment of 1. Selective ^{13}C enrichement of **1** at the α-carbon was achieved by following the above procedure for the synthesis of ^{13}C-enriched $[Ru_3(*CO)_9*C*CO]^{2-}$, but after acylation (before the second reduction step) the THF solution of $[Ru_3(*CO)_{10}(\mu\text{-}*COC(O)CH_3)]^-$ was stirred under an atmosphere of ^{12}CO for 15 min. The exchanged atmosphere was removed and replaced with fresh ^{12}CO and the solution stirred for another 15 min. This procedure was repeated several times, which resulted in the isotopic dilution of all 10 of the terminally bound CO ligands while the $(\mu\text{-}*COC(O)CH_3)$ moiety was left unexchanged. Reductive cleavage of the acetate function and subsequent workup as described above gave $[Ru_3(CO)_9*CCO]^{2-}$. The extent of

(1) Sailor, M. J.; Shriver, D. F. *Organometallics* **1985**, *4*, 1476.
(2) Kolis, J. W.; Holt, E. M.; Shriver, D. F. *J. Am. Chem. Soc.* **1983**, *105*, 7307.
(3) Sievert, A. C.; Strickland, D. S.; Shapley, J. R.; Steinmetz, G. R.; Geoffroy, G. L. *Organometallics* **1982**, *1*, 214.
(4) Seyferth, D.; Williams, G. H.; Nivert, C. L. *Inorg. Chem.* **1977**, *16*, 758.
(5) Holmgren, J. S.; Shapley, J. R. *Organometallics* **1984**, *3*, 1322.
(6) Shriver, D. F.; Drezdzon, M. A. *Manipulation of Air Sensitive Compounds*; Wiley: New York, 1986.
(7) Gordon, A. J.; Ford, R. A. *The Chemist's Companion*; Wiley: New York, 1972.
(8) Bruce, M. I.; Matisons, J. G.; Wallis, R. C.; Patrick, J. M.; Skelton, B. W.; White, A. H. *J. Chem. Soc., Dalton Trans.* **1983**, 2365.
(9) The "chloro adduct" here is assumed to be predominantly $[Ru_3(C-O)_{11}(C(O)Cl)]^-$ (**9**) based on the similarity of its infrared spectrum to the previously characterized $[Ru_3(CO)_{11}(CO_2CH_3)]^-$.[10] Formation of $[Ru_3(\mu\text{-}Cl)(CO)_{10}]^-$ is also a possibility under these conditions,[11] but we see no evidence for its formation in the infrared spectrum. For **9**: IR (ν_{CO}, THF) 2102 (w), 2063 (m), 2030 (vs), 2015 (vs), 1996 (m), 1978 (m sh), 1965 (s), 1911 (w), 1881 (w), 1831 (s), 1776 (w) cm^{-1}. It is important to form the chloro adduct before adding the reducing agent because any excess $Ru_3(CO)_{12}$ present will instantly react with the $[Ru_3(CO)_{11}]^{2-}$ formed to produce $[Ru_4(CO)_{13}]^{2-}$.[12]
(10) Gross, D. C.; Ford, P. C. *J. Am. Chem. Soc.* **1985**, *107*, 585.
(11) Lavigne, G.; Kaesz, H. D. *J. Am. Chem. Soc.* **1984**, *106*, 4697.
(12) Bhattacharyya, A. A.; Nagel, C. C.; Shore, S. G. *Organometallics* **1983**, *2*, 1187.
(13) *International Tables for X-ray Crystallography*; Kynoch: Birmingham, England, 1974; Vol. IV.

enrichment and isotopic dilution was checked by ^{13}C NMR.

Selective ^{13}C enrichment at only the α- and the β-carbon of the CCO was achieved in the following manner: The compound $[PPN]_2[Ru_3(*CO)_9(*C*CO)]$ (200 mg, ^{13}C enriched to ca. 30%) was dissolved in 10 mL of acetone and placed in a 100-mL capacity autoclave. The apparatus was purged twice and pressurized to 900 psi with ^{12}CO and heated at 70–80 °C for 3 h. The autoclave was cooled and vented and the product syringed out. Crystallization by addition of 10 mL of Et_2O yielded $[PPN]_2[Ru_3(CO)_9*C*CO]$ in near quantitative yield. ^{13}C NMR indicated that the metal-bound carbonyl ligands of the product had become depleted in ^{13}C to the level of natural abundance, while a slight depletion had also occurred at the β-position of the CCO ligand, indicating that this CO is exchanged at a much slower rate. Compound **1** does not exchange with an atmosphere of ^{12}CO in the presence of [PPN]I or [PPN]Cl in CH_2Cl_2 solution, nor does it exchange in THF solution in the presence of a catalytic amount of Na/benzophenone ketyl solution. In refluxing acetonitrile under a ^{12}CO atmosphere **1** slowly exchanges (ca. 3–5 days) all carbonyl ligands (including the CCO), although under these conditions depletion of the CCO carbonyl is three times slower than the metal-bound carbonyls (as determined by ^{13}C NMR spectroscopy).

Preparation of [PPN][$HRu_3(CO)_9(\mu_3$-CCO)] (2). A 100-mg (0.06-mmol) sample of (1) was dissolved in 4 mL of CH_2Cl_2, and the solution was cooled to −78 °C. A 5.3-μL (0.06-mmol) aliquot of HSO_3CF_3 was added by microliter syringe, and the cooling bath was removed. The solution was stirred as it warmed to room temperature. Diethyl ether (20 mL) was added, the mixture was filtered, and the yellow-orange filtrate was pumped to dryness. The residue was recrystallized from diethyl ether/pentane. Slow diffusion produced small yellow crystals, which were isolated in 41% yield (28 mg): IR (ν_{CO}, Et_2O) 2069 (w), 2032 (s), 2017 (m), 1999 (vs), 1969 (m), 1927 (w) cm^{-1}; ^1H NMR (CD_2Cl_2, 25 °C) −17.51 (s) ppm; ^{13}C NMR (THF-d_8, −90 °C) 205.3, 196.1 (br, 3:6 terminal CO's); 165.1 (*C*CO, $^1J_{CC}$ = 78 Hz), 50.1 (*C*CO, $^1J_{CC}$ = 78 Hz) ppm. Anal. Calcd (Found) for $C_{47}H_{31}NO_{10}P_2Ru_3$: C, 49.74 (48.93); H, 2.75 (2.69); N, 1.23 (1.17); Ru, 26.72 (25.78).

Preparation of $H_2Ru_3(CO)_9(\mu_3$-CCO) (3). A solution of 100 mg (0.06 mmol) of **1** in 4 mL of CH_2Cl_2 was stirred rapidly while 0.2 mL (3 mmol) of 85% H_3PO_4 was added. The mixture was stirred for 20 min. Pentane (20 mL) was added and the mixture filtered. The yellow filtrate was pumped dry and the residue extracted into pentane. The volume of the resulting yellow solution was reduced to ca. 1 mL under a fast dinitrogen stream. Yellow crystals formed that were separated from the supernatant and dried in vacuo; 16 mg (45% yield) was isolated: IR (ν_{CO}, pentane) 2123 (vw), 2088 (s), 2062 (vs), 2043 (w), 2017 (m), 2008 (w), 1969 (vw); ^1H NMR (CD_2Cl_2) −17.99 ppm; ^{13}C NMR (CD_2Cl_2, −90 °C) 182.8, 186.2, 190.3, 194.8, 198.9 (2:2:1:2:2, terminal CO's), 158.8 (*C*CO, $^1J_{CC}$ = 78 Hz), 38.7 (*C*CO, $^1J_{CC}$ = 78 Hz) ppm; mass spectrum (70 eV, EI), *m/e* 599 (parent), indiscriminate loss of 10 CO's and two H's. MASSPAN analysis of the isotopic distribution in the parent envelope obtained with 15-eV accelerating voltage gives R = 5.2% for formula **3**.

Preparation of [PPN][$Ru_3(CO)_{10}(\mu_3$-CC(O)CH_3)] (4). A solution of 200 mg (0.12 mmol) of **1** in 10 mL of dichloromethane was put under an atmosphere of CO in a 100-mL Schlenk flask. Methyl iodide (0.2 mL, 3.2 mmol) was added by syringe under a CO purge. The flask was covered with foil and stirred for 24 h. The solvent was removed and the product extracted into 60 mL of diethyl ether. The solution was filtered and the volume of the yellow filtrate slowly reduced by pumping. Yellow microcrystals resulted that were dried in vacuo; 50 mg (36% yield) were isolated. ^1H NMR showed that the PPN^+ salt of **4** crystallizes with one molecule of diethyl ether per formula unit: IR (ν_{CO}, CH_2Cl_2) 2032 (vs), 1988 (s), 1660 (w), 1590 (w) cm^{-1}; IR (KBr, Nujol mull) 2072 (w), 2025 (vs), 1972 (vs, br), 1679 (s, μ-CO), 1590 (m, C=O); ^1H NMR (CD_2Cl_2) 2.34 (s, CH_3) ppm (resonances for Et_2O); ^{13}C NMR (CD_2Cl_2, −90 °C) 273.3 (μ-CO), 212.7 (*C*C(O)Me, $^1J_{CC}$ = 44 Hz), 198.7 (terminal CO's), 191.8 (*C*C(O)Me, $^1J_{CC}$ = 44 Hz) ppm. The reaction was also carried out with 25% $^{13}CH_3I$, which yielded the additional ^{13}C NMR coupling data: 212.7 (*C*C(O)CH_3, $^1J_{CC}$ = 42 Hz), 191.9 (*C*C(O)CH_3, $^2J_{CC}$ = 20 Hz), 31.3 (CC(O)*C*H_3, $^1J_{CC}$ = 42 Hz, $^2J_{CC}$ = 20 Hz) ppm. The proton-coupled ^{13}C spectrum provided the following data: 31.3 (q, CC(O)*C*H_3, $^1J_{CH}$ = 127 Hz) ppm. The ^{13}C spectra of **4** indicate that in the course of the synthesis the ^{13}C-enriched terminal carbonyl ligands have partially exchanged with the ^{12}CO used during the methylation step. Anal. Calcd (Found) for $C_{53}H_{43}NO_{12}P_2Ru_3$: C, 50.88 (50.14); H, 3.46 (3.41); N, 1.12 (1.17); Ru, 24.24 (22.46).

Reaction of $[Ru_3(CO)_9(*C*CO)]^{2-}$ with CH_3I. The normal procedure for the synthesis of **4** was followed, but a ^{13}C-enriched sample of $[PPN]_2[Ru_3(CO)_9(*C*CO)]$ (30% ^{13}C at α-C, 20% ^{13}C at β-C, <2% ^{13}C at metal-bound CO's, prepared as described above) was used. The ^{13}C NMR spectrum of the product **4** contained resonances for the α-carbon and the nine equivalent CO ligands, but the signal for the acyl CO of the $CC(O)CH_3$ ligand was unobservable. The signal to noise ratio in the spectrum was 35 (based on the α-carbon resonance). Therefore the upper limit for the percent ^{13}C enrichment of the acyl CO carbon is 1.7%, based on a detection limit of 2σ and an α-carbon resonance which is 30% ^{13}C. Since the identical reaction using $[Ru_3(*CO)_9(\mu_3$-*C*CO)]$^{2-}$ (30% ^{13}C enriched at all carbon atoms) as the starting material results in product **4** which contains both the α-carbon and acyl carbon resonances of the $CC(O)CH_3$ moiety in approximately 1:1 intensity ratio in the ^{13}C NMR spectrum, the origin of the acyl carbonyl is unequivocally established as being a metal-bound CO on the starting material $[Ru_3(CO)_9(\mu_3$-CCO)]$^{2-}$. Furthermore, scrambling of the CCO carbonyl with the metal-bound carbonyls *prior* to formation of the $C(O)-CH_3$ bond is ruled out because this would give rise to a level of enrichment of at least 2.9% on the acyl carbonyl.

Preparation of $Ru_3(CO)_9(\mu_3$-CO)(μ_3-CC(OMe)Me) (5). A solution of 100 mg (0.06 mmol) of **1** in 5 mL of CH_2Cl_2 was placed under a CO atmosphere and 0.3 mL (2.7 mmol) of $CH_3OSO_2CF_3$ introduced under a CO purge. The resulting yellow-orange solution was stirred for 25 min. At this point, 20 mL of pentane was added to the red-orange solution and a white precipitate of $PPNSO_3CF_3$ separated out. The mixture was filtered and the filtrate pumped dry. The residue was extracted into 20 mL of pentane and filtered, and the volume of the extract was slowly reduced to ca. 1 mL by vacuum. The resulting orange crystals were separated from the supernatant and dried in vacuo: yield 14 mg, 24%; IR (ν_{CO}, pentane) 2093 (w), 2061 (vs), 2041 (s), 2024 (s), 2004 (m, sh), 1918 (w, br) cm^{-1}; IR (KBr pellet) 2094 (m), 2062 (vs), 2046 (vs), 2026 (vs), 2022 (vs), 1995 (vs), 1979 (s), 1683 (s, μ_3-CO), 1495 (m, C=C) cm^{-1}; ^1H NMR (CD_2Cl_2) 3.81 (s, OC*H*$_3$), 2.36 (s, CC(OCH$_3$)C*H*$_3$) ppm; ^{13}C NMR (CD_2Cl_2, −90 °C) 263.0 (br, μ_3-CO), 195.6 (terminal CO's); 192.8 (*C*C(OCH$_3$)CH$_3$, $^1J_{CC}$ = 55 Hz), 168.7 (*C*C(OCH$_3$)CH$_3$, $^1J_{CC}$ = 55 Hz), 58.5 (CC(O*C*H$_3$)CH$_3$), 27.2 (CC(OCH$_3$)*C*H$_3$) ppm; mass spectrum (70 eV, EI), *m/e* 655 (parent), successive loss of 10 CO's. MASSPAN analysis of the isotopic distribution in the parent ion envelope gives R = 12.9% for the formula $Ru_3(CO)_{10}$(CC(OMe)Me).

Preparation of $H_2Ru_3(CO)_9(\mu_3$-CC(OMe)Me) (6). To a 100-mL Schlenk flask containing 15 mg (0.02 mmol) of **3** was added 10 mL of pentane. H_2 (ca. 1 atm) was introduced, and the mixture was stirred for 12 h. Orange yellow crystals (12 mg, 90% yield) were obtained by slow cooling and evaporation of solvent under a fast dinitrogen stream: IR (ν_{CO}, pentane) 2106 (w), 2078 (s), 2054 (vs), 2044 (s), 2016 (s), 2005 (m), 1990 (m) cm^{-1}; ^1H NMR (CD_2Cl_2, 25 °C) 3.62 (s, 3 H, CC(OC*H*$_3$)CH$_3$), 2.51 (s, 3 H, CC(OCH$_3$)C*H*$_3$), −17.77 (s, 1.3 H, μ-H) ppm; ^{13}C NMR (CD_2Cl_2, −90 °C) 214.2 (br, *C*C(OCH$_3$)CH$_3$), 197.9, 196.3, 191.8, 188.3, 186.9 (2:2:1:2:2, terminal CO's), 149.8 (*C*C(OCH$_3$)CH$_3$, $^1J_{CC}$ = 50 Hz), 57.6 (CC(O*C*H$_3$)CH$_3$), 27.8 (CC(OCH$_3$)*C*H$_3$) ppm; ^{13}C NMR (CD_2Cl_2, −30 °C) 213.6 (*C*C(OCH$_3$)CH$_3$, $^1J_{CC}$ = 50 Hz), 198, 188 (br, terminal CO's), 151.6 (*C*C(OCH$_3$)CH$_3$, $^1J_{CC}$ = 50 Hz), 57.8 (CC(O*C*H$_3$)CH$_3$), 27.9 (CC(OCH$_3$)*C*H$_3$) ppm; mass spectrum (70 eV, EI), *m/e* 629 (parent), indiscriminate loss of nine CO's and two H's. MASSPAN analysis of the isotopic distribution in the parent envelope gives R = 6.8% for the formula of **6**.

Reactions of 2 and 3 with $LiCH_3$. In both cases ca. 0.06 mmol of cluster was dissolved in 10–20 mL of diethyl ether and the solution cooled to −78 °C in an acetone/dry ice bath. One equivalent of $LiCH_3$ (1.2 M solution in ether) was added slowly by syringe. In the case of **2**, a yellow-brown precipitate formed on warming to room temperature which was isolated and washed with diethyl ether. The solid was dried and dissolved in 4 mL of CH_2Cl_2, and 2 drops of 85% H_3PO_4 was added to the solution. After 10 min of stirring, pentane (40 mL) was added and the yellow-brown slurry was filtered. The solvent was removed from the filtrate by vacuum and the residue extracted into pentane. Filtration and removal of solvent yielded $H_2Ru_3(CO)_9(\mu_3$-η^2-CHC(O)CH_3) (7): IR (ν_{CO}, pentane) 2110 (m), 2083 (s), 2059 (vs), 2038 (s), 2023 (m), 2011 (s), 1996 (m) cm^{-1}; IR (KBr) 2108 (m), 2078 (s), 2044 (vs), 2029 (s), 1997 (vs), 1970 (m), 1921 (w), 1513 (w, η^2-C=O) cm^{-1}; ^1H NMR (CD_2Cl_2, −30 °C) 4.16 (s, 1 H, C*H*C(O)CH$_3$), 1.99 (s, 3 H, CHC(O)C*H*$_3$), −12.64 (d, 1 H, J_{HH} = 3 Hz), −14.44 (d, 1 H, J_{HH} = 3 Hz) ppm; ^{13}C NMR (CD_2Cl_2, −90 °C) 239.5 (CH*C*(O)CH$_3$, $^1J_{CC}$ = 43 Hz), 201.4, 197.6, 197.3, 197.0, 190.3, 188.4, 185.1, 184.6, 182.9 (9 terminal CO's), 74.3 (*C*HC(O)CH$_3$, $^1J_{CC}$ = 43 Hz, in the proton-coupled spectrum the resonance splits into a doublet, $^1J_{CH}$ = 143 Hz, $^1J_{CH}$ satellites of 143 Hz were also observed in the ^1H NMR spectrum on the 4.16 ppm resonance) ppm; mass spectrum (70 eV, EI). *m/e* 615 (parent). MASSPAN analysis of the isotope distribution in the parent ion envelope yields R = 8.1% fit for formula **7**. The product of the reaction of **3** with $LiCH_3$ was reacted directly with excess $CH_3OSO_2CF_3$. After being stired for 4 h at room temperature, the solution was pumped dry and the residue extracted with pentane. The yellow product was identified as $H_2Ru_3(CO)_9(\mu_3$-CC(OCH$_3$)CH$_3$) (**6**) by infrared and ^1H NMR spectra.

X-ray Crystallographic Solution of 5. The relevant data collection and crystal parameters are summarized in Table II. A suitable crystal was

Table II. Summary of Crystal Data and Intensity Collection for Compound **5**

system	monoclinic
space group	$P2_1/n$
a, Å	8.3993 (17)
b, Å	15.9259 (16)
c, Å	14.1140 (13)
β, deg	90.95 (1)
V, Å^3	1887.73
formula	$C_{14}H_6Ru_3O_{11}$
fw	653
Z	4
μ(Mo Kα), cm^{-1}	23.8
d_{calcd}, g/cm^3	2.296
cryst size, mm	0.3 × 0.3 × 0.3
diffractometer	Enraf-Nonius CAD-4
radiation	Mo Kα (monochromated)
scan method (quadrants)	ω–2θ (h,k,±l)
data collectn range, deg.	3–55 (2θ)
unique data	4315
unique data, $I > 3\sigma(I)$	4067
no. of parameters refined	254
R	0.0253
R_w	0.0522
error in observn of unit wt	1.883
largest shift/error, final cycle	0.01
abs cor	empirical, Ψ scan
transmissn range	90.8–99.9
temp, °C	−100

obtained by slow cooling of a concentrated hexane solution of **5**. Calculations were carried out by using the Enraf-Nonius SDP crystallographic computing package. The data were corrected for Lorentz and polarization effects. The structure was solved via Patterson synthesis, which yielded the positions of the three ruthenium atoms. Subsequent Fourier syntheses revealed the locations of all remaining non-hydrogen atoms. Idealized hydrogen atom positions were calculated and included in the structure factor calculation but not refined. The structure was refined by using full-matrix least-squares techniques based on minimizing $\sum\omega(F_o - F_c)^2$, where ω is based on counting statistics modified by an ignorance factor, $p = 0.05$. Scattering factors and corrections for anomalous dispersion were taken from the literature.[13] All non-hydrogen atoms were refined anisotropically. Several of the systematically absent reflections for the space group $P2_1/n$ were obserbed to have $I \geq 3\ \sigma(I)$. The Friedel pairs of these reflections were all unobservable, indicating that these peaks were caused by secondary diffraction. Successful solution and refinement of the structure in $P2_1/n$ supports this choice of space group.

Extended Hückel Calculations. The calculations were performed by using the program ICON8.[14] Values for the diagonal matrix elements and orbital exponents were taken from the literature.[15] The geometry for **1** was idealized to C_{3v} symmetry, with bond distances based on the average bond distances in the crystal structure of **1**. In all three cases, the capping CCO ligand was placed in a vertical orientation with the α-carbon 2.16 Å from each metal vertex. The C_α–C_β distance was taken as 1.30 Å. All carbon-oxygen distances were taken as 1.17 Å, and all metal to terminal carbonyl carbon distances were set at 1.87 Å. The geometries of **2** and **3** were idealized as C_s, with six axial and three equatorial carbonyl ligands and the bridging hydrides placed symmetrically 2.07 Å from two metal atoms, 0.3 Å below the plane of the metals.

Results and Discussion

Reactivity of $[Ru_3(CO)_9(\mu_3\text{-}CCO)]^{2-}$. Reaction of $[PPN]_2[Ru_3(CO)_9(\mu_3\text{-}CCO)]$ (**1**) with excess CH_3I under a CO atmosphere results in formation of the acetyl cluster $[Ru_3(CO)_{10}(\mu_3\text{-}CC(O)CH_3)]^-$ (**4**) in good yield (Scheme I). Further alkylation of **4** with methyl trifluoromethanesulfonate leads to attack at the acyl oxygen to give the vinylidene complex $Ru_3(CO)_{10}(\mu_3\text{-}CC(OCH_3)CH_3)$ (**5**) exclusively. This compound has been characterized by mass spectroscopy, ^{13}C, and ^1H NMR spectroscopy, and single-crystal X-ray diffraction. The transformation

Scheme I

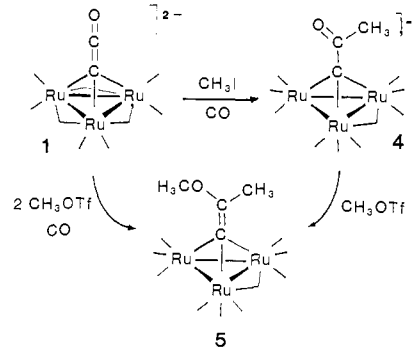

Scheme II

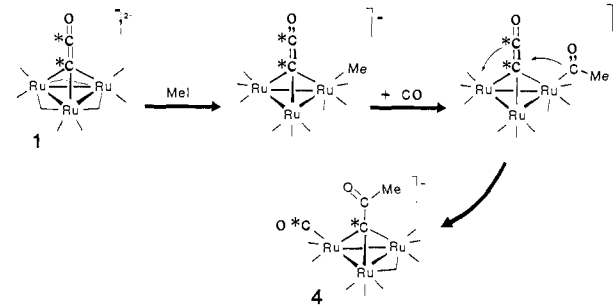

1 → **4** → **5** represents the addition of 2 equiv of CH_3^+ to convert a ketenylidene ligand into an enol ether vinylidene. The conversion can be effected directly by addition of excess $CH_3OSO_2CF_3$ to **1** under a CO atmosphere, as shown in Scheme I.

The products appear to be the result of direct attack by CH_3^+ on the β-carbon of the CCO ligand. Such an outcome is totally unexpected on the basis of previous studies of ketenylidene reactivity,[2-4,16,17] analogy to organic ketene chemistry, and charge densities from the extended Hückel calculations, which are described below. The possibility of an indirect alkylation mechanism was therefore considered. To test this idea, ^{13}C-labeling experiments were performed in order to establish the origin of the acyl CO in $[Ru_3(CO)_{10}(\mu_3\text{-}CC(O)CH_3)]^-$ (**4**). As shown in Scheme II the selectively ^{13}C-enriched ketenylidene $[Ru_3(CO)_9(\mu_3\text{-}*C*CO)]^{2-}$ reacts with methyl iodide to produce **4** which does not contain the label at the acyl carbonyl. Thus direct attack by CH_3^+ at the β-carbon of the CCO is ruled out. In a separate experiment, $[Ru_3(CO)_9(\mu_3\text{-}CCO)]^{2-}$ which has been ^{13}C-enriched at all carbons was alkylated and the resulting product **4** contains a ^{13}C label at the acyl CO. In both cases the reactions were carried out under a ^{12}CO atmosphere. These observations lead to the conclusion that the acyl CO originates from a metal-bound carbonyl ligand. The data are in agreement with the mechanism proposed in Scheme II, in which initial attack by CH_3^+ occurs at a metal center. This is followed by migratory insertion of CO into the metal–carbon σ bond, a well-known organometallic reaction[18a] which also has precedent in metal cluster chemistry.[18b] The product **4** is then generated by migration of the acyl group to the α-carbon of the CCO concomitant with migration of the CCO carbonyl down to the metal framework.

In contrast to the ruthenium ketenylidene **1**, the anionic ketenylidenes $[Fe_3(CO)_9(\mu_3\text{-}CCO)]^{2-}$ and $[CoFe_2(CO)_9(\mu_3\text{-}CCO)]^-$ are attacked directly by electrophiles such as CH_3^+ or H^+ at the α-carbon with concomitant migration of the ketenyl CO (the β-carbon) onto the metal framework.[2,16] Therefore a recurring theme in the chemistry of the anionic ketenylidenes is the ready

(14) ICON8 is QCPE program No. 344, Chemistry department, Indiana University, Bloomington, Ind.

(15) (a) H, C, and O parameters are from: Schilling, B. E. R.; Hoffmann, R. *J. Am. Chem. Soc.* **1979**, *101*, 3456. (b) Ru parameters are from: Thorn, D. L.; Hoffmann, R. *Inorg. Chem.* **1978**, *17*, 126.

(16) Kolis, J. W.; Holt, E. M.; Hriljac, J. A.; Shriver, D. F. *Organometallics* **1984**, *3*, 496.

(17) Hriljac, J. A.; Shriver, D. F. *Organometallics* **1985**, *4*, 2225.

(18) (a) Collman, J. P.; Hegedus, L. S. *Principles and Applications of Organotransition Metal Chemistry*; University Science Books: Oxford, 1980. (b) Morrison, D.; Bassner, S. L.; Geoffroy, G. L. *Organometallics* **1986**, *5*, 408.

Scheme III

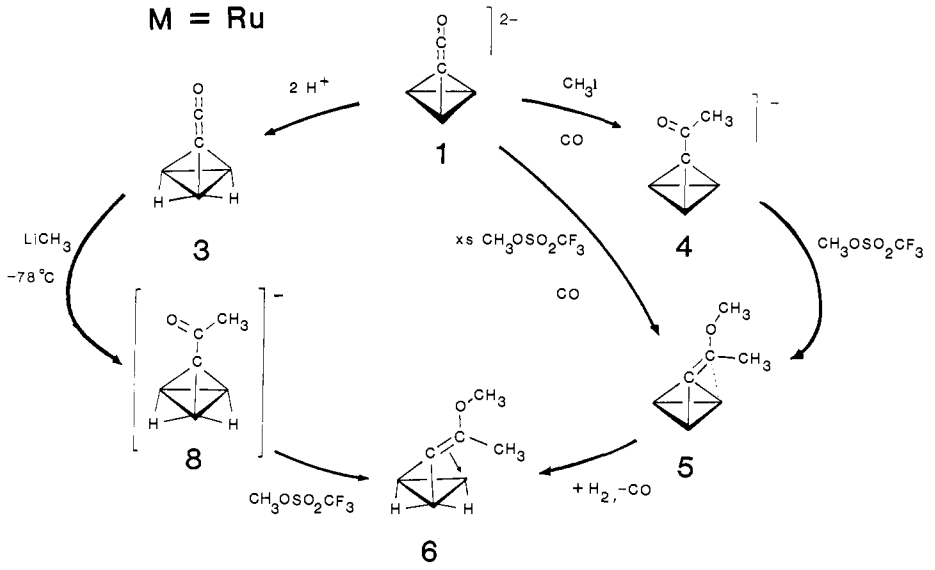

cleavage of the C=C bond of the CCO ligand. In the ketenylidenes made up of first-row elements the cleavage is most readily achieved, while the second-row ruthenium ketenylidene requires activation via a migrating acyl group to effect cleavage of the C=C bond. The tendency for C_α–C_β cleavage is also reflected in ^{13}C exchange experiments. Under a ^{13}CO atmosphere both $[Fe_3(CO)_9(\mu_3\text{-}CCO)]^{2-}$ and $[CoFe_2(CO)_9(\mu_3\text{-}CCO)]^-$ readily exchange all ten carbonyl groups (including the β-carbon of the CCO).[2,19] By contrast, the ruthenium ketenylidene $[Ru_3(CO)_9(\mu_3\text{-}CCO)]^{2-}$ (**1**) requires more forcing conditions to effect CO exchange, and the exchange of the CCO carbonyl occurs on a much slower time scale then the metal-bound carbonyls (see Experimental Section).

$$[Ru_3(^*CO)_9(^*C^*CO)]^{2-} \xrightarrow[60\ atm,\ 70\ °C]{^{12}CO} [Ru_3(CO)_9(^*C^*CO)]^{2-}$$

Alkylation of **1** results in the formation of products **4** and **5** which contain one more carbonyl ligand than the starting material. This CO uptake is required to maintain the 48 cluster-valence-electron count on the cluster because the formal 6e donor $[CCO]^{2-}$ is converted into the 4e donors $[C{-}C(O)CH_3]^-$ or $C{=}C(OMe)CH_3$. The reaction of **1** with CH_3I or $CH_3OSO_2CF_3$ also occurs under a nitrogen atmosphere, but in the absence of CO the reactions do not proceed cleanly. Apparently in the absence of gaseous CO the extra CO needed to form **4** is derived from cluster decomposition.

The vinylidene cluster **5** undergoes a facile substitution reaction with H_2, resulting in the addition of H_2 to the metal framework and the elimination of CO to form $H_2Ru_3(CO)_9(\mu_3\text{-}CC(OMe)Me)$ (**6**). The reaction proceeds to completion under mild conditions (1 atm of H_2 at room temperature in 12 h).

Reactivity of $[HRu_3(CO)_9(\mu_3\text{-}CCO)]^-$ and $H_2Ru_3(CO)_9(\mu_3\text{-}CCO)$. As indicated by the ^{13}C NMR data and infrared spectra, addition of H^+ to $[Ru_3(CO)_9(\mu_3\text{-}CCO)]^{2-}$ (**1**) results in a shift of three bridging CO ligands to terminal positions in **2** and **3**. The C_α–C_β ^{13}C coupling constant decreases from 96 to 78 Hz upon protonation. There is no further change in the coupling constant on addition of a second proton to $[HRu_3(CO)_9(\mu_3\text{-}CCO)]^-$ (i.e., $^1J_{CC}$ for $H_2Ru_3(CO)_9(\mu_3\text{-}CCO)$ is 78 Hz). These data demonstrate that a major structural change occurs on the conversion of the doubly negative cluster **1** to the mononegative **2** but relatively little change occurs upon the protonation of **2** to yield **3**. The first protonation also is the point at which the CCO ligand changes from a nucleophile to an electrophile.

Both $[HRu_3(CO)_9(\mu_3\text{-}CCO)]^-$ (**2**) and $H_2Ru_3(CO)_9(\mu_3\text{-}CCO)$ (**3**) are attacked by the nucleophile $LiCH_3$ at the β-carbon of the CCO ligand. In the case of **2**, workup in acid solution produces $H_2Ru_3(CO)_9(\mu_3\text{-}\eta^2\text{-}CHC(O)CH_3)$ (**7**), the result of nucleophilic attack of the β-carbon by CH_3^- followed by electrophilic attack at the α-carbon by H^+. Compound **7** is spectroscopically

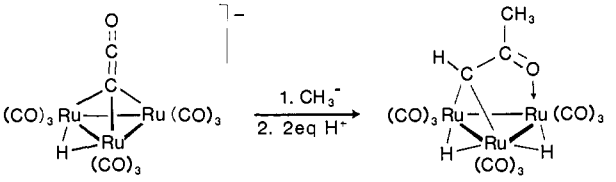

2 **7**

analogous to $H_2Ru_3(CO)_9(\mu_3\text{-}\eta^2\text{-}CHC(O)OCH_3)$, which has been crystallographically characterized.[20] The very low ν_{CO} frequency of 1513 cm^{-1} in **7** is indicative of an interaction of the acetyl oxygen with a metal vertex.

The ketenylidene cluster $H_2Ru_3(CO)_9(\mu_3\text{-}CCO)$ (**3**), previously synthesized by an alternate route,[5] is readily attacked by nucleophiles at the β-carbon.[5] Hence reaction of **3** with $LiCH_3$ at −78 °C generates the intermediate **8**, which can then be treated with $CH_3OSO_2CF_3$ to generate $H_2Ru_3(CO)_9(\mu_3\text{-}CC(OMe)Me)$ (**6**) (Scheme III). Therefore, the vinylidene **6** can be synthesized from $[Ru_3(CO)_9(\mu_3\text{-}CCO)]^{2-}$ (**1**) by two routes, involving either electrophilic or nucleophilic attack on a ketenylidene cluster. Control over the character of the ketenylidene in these reactions is achieved by protonation of the cluster framework. Nucleophilic attack at the β-carbon of the $(\mu_3$-CCO) ligand is known to occur in $H_2M_3(CO)_9(\mu_3\text{-}CCO)$ (M = Ru, Os),[3,5] $[Co_3(CO)_9(\mu_3\text{-}CCO)]^+$,[4] and $[Fe_2Co(CO)_9(\mu_3\text{-}CCO)]^-$.[19]

Bonding. Extended Hückel calculations were performed on the series of ketenylidenes $[Ru_3(CO)_6(\mu\text{-}CO)_3(\mu_3\text{-}CCO)]^{2-}$ (**1**), $[HRu_3(CO)_9(\mu_3\text{-}CCO)]^-$ (**2**), and $H_2Ru_3(CO)_9(\mu_3\text{-}CCO)$ (**3**) in an attempt to discern the factors involved in their differing reactivities. The molecular orbitals of **2** and **3** are qualitatively very similar because the ligand geometries are similar. The results and conclusions of the calculations on either **2** or **3** are therefore essentially the same. However, the structure of **1** contains three symmetrically bridging carbonyls, and this different ligand environment is reflected in a different form for the molecular orbitals.

Each of the molecules **1**, **2**, and **3** has a set of three lowest unoccupied orbitals within 0.2 eV of each other. Likewise the extended Hückel calculations show a set of three highest occupied

(19) Ching, S.; Holt, E. M.; Kolis, J. W.; Shriver, D. F., submitted for publication.

(20) Churchill, M. R.; Janik, T. S.; Duggan, T. P.; Keister, J. B. *Organometallics* **1987**, *6*, 799.

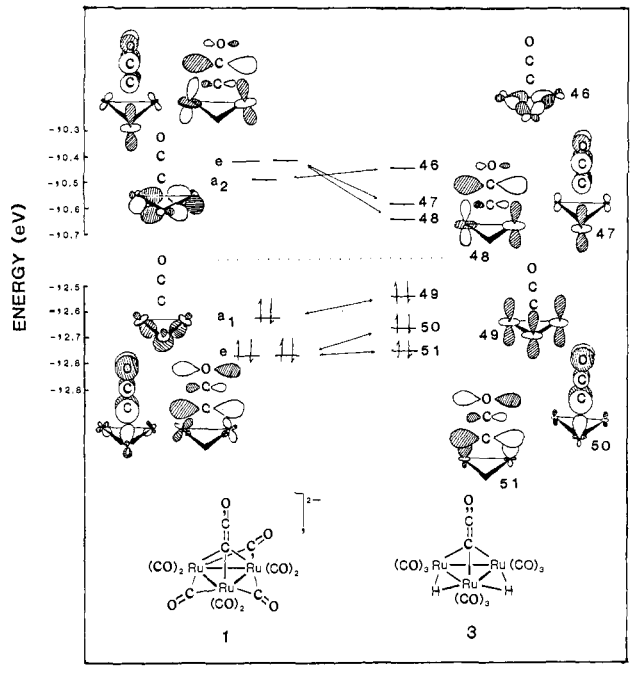

Figure 1. Schematic representation of the frontier orbitals for the series of ketenylidene $[Ru_3(CO)_6(\mu\text{-}CO)_3(CCO)]^{2-}$, $[HRu_3(CO)_9(CCO)]^-$, and $H_2Ru_3(CO)_9(CCO)$.

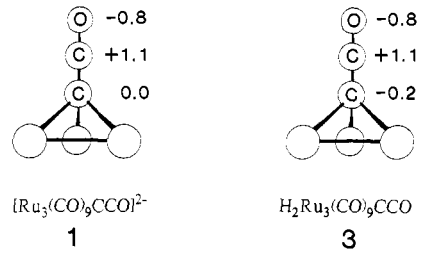

Figure 2. Distribution of partial charges on the CCO ligand obtained from the EHMO calculations for $[Ru_3(CO)_6(\mu\text{-}CO)_3(CCO)]^{2-}$ (**1**) and $H_2Ru(CO)_9(CCO)$ (**3**).

orbitals that are very close energetically, as depicted in Figure 1. The energetic proximity of the orbitals complicates the interpretation somewhat, as any one of the set of three orbitals may be involved in determining the reactivity of the molecule. Hence for either geometry there is a total of six orbitals which should be considered in interpreting the electrophilic or nucleophilic behavior of the molecule. The HOMO - LUMO energy difference in all three molecules is ca. 2 eV, with the largest gap occurring in **1**. The HOMOs in either case are bonding orbitals involving metal–metal, metal–carbonyl, and metal–α-carbon interactions. Each set of LUMOs is metal–metal antibonding, and C_α–C_β bonding.

For compounds **2** and **3** the LUMOs have a large orbital coefficient on C_β, indicating potential electrophilic character at this site. This reactivity pattern was observed for the β-carbon of compounds **2** and **3**. In contrast, the LUMO of **1** is an antibonding orbital based mostly on the metals of the framework, and therefore attack by a nucleophile on the β-carbon of **1** is not predicted by the calculations. This is in agreement with the experimental observations.[1] The tendency toward nucleophilic addition appears to be controlled by the charge on the cluster. The dianion **1** does not react with anionic nucleophiles whereas the monoanion **2** and the neutral cluster **3** do.

The interaction of the series of ketenylidenes with electrophiles is more complicated. Under mild conditions only the dinegative ketenylidene **1** is observed to react with the strong alkylating agent $CH_3OSO_2CF_3$, resulting in the apparent addition of a methyl group to the β-carbon of the CCO. As shown in Figure 1, the HOMO of **1** is primarily based on the metal framework. Also, the distribution of partial charges about the molecule indicates

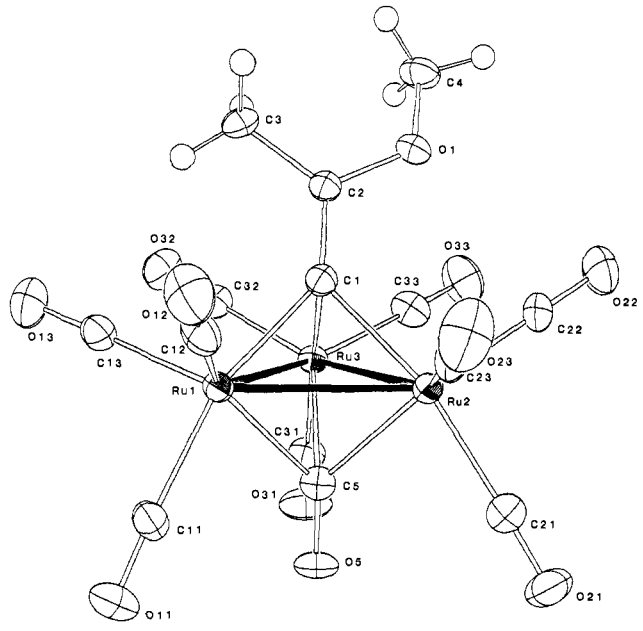

Figure 3. ORTEP drawing of $Ru_3(CO)_9(\mu_3\text{-}CO)(\mu_3\text{-}C{=}C(OCH_3)CH_3)$ (**5**). Thermal ellipsoids are drawn at 50% probability level.

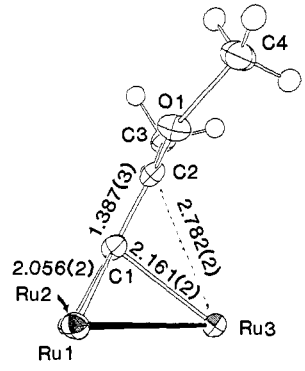

Figure 4. ORTEP drawing of the $Ru_3(C{=}C(OCH_3)CH_3)$ moiety of **5** showing the near planarity of the vinylidene group. Note the C2–Ru3 vector is not within bonding distance.

that the metals carry most of the negative charge and the β-carbon is the most positively charged atom in the molecule (Figure 2). Therefore, the Hückel calculation suggests that the β-carbon is the least likely site of electrophilic attack in either a charge-controlled or orbital-controlled fashion, and so direct attack at the β-position is not predicted by the calculations. On the other hand, the existence of the metal-based HOMO of **1** lends support to the postulate presented in Scheme II that initial attack by a methyl group occurs at the metal framework.

Structure of $[Ru_3(CO)_9(\mu_3\text{-}CO)(\mu_3\text{-}C{=}C(OCH_3)CH_3)]$ (5). The compound exists in the solid state as one discrete molecule per asymmetric unit. The ruthenium framework forms an approximately isosceles triangle with all three ruthenium–ruthenium vectors shortened with respect to those observed in $Ru_3(CO)_{12}$[21] by ca. 0.07 Å. This is to be expected from the presence of the two capping ligands. Appropriate bond distances and angles are presented in Table IV. A diagram of **5** showing the atom numbering scheme is presented in Figure 3.

An especially interesting structural feature of **5** is the disposition of the capping vinylidene ligand. This ligand appears to have sp^2 hybridization around the central carbon atoms. The $Ru_2C{=}C$-(OMe)Me array is nearly planar (Figure 4), and the maximum deviation of the $Ru_2C{=}C(OC)C$ moiety is 0.036 (3) Å from the least-squares plane containing these atoms. Additionally, the bond angle of O1–C2–C3 (Figure 3) is 118.2 (2)°, just slightly smaller

(21) Churchill, M. R.; Hollander, F. J.; Hutchinson, J. P. *Inorg. Chem.* **1977**, *16*, 2655.

Table III. Positional Parameters and Their Estimated Standard Deviations for $Ru_3(CO)_{10}(\mu_3$-CC(OMe)Me) (**5**)[a]

atom	*x*	*y*	*z*	*B*, Å^2
Ru1	0.04871 (3)	0.33976 (1)	0.64904 (2)	1.372 (4)
Ru2	0.33434 (3)	0.33854 (1)	0.75302 (2)	1.409 (4)
Ru3	0.12761 (3)	0.20321 (1)	0.76263 (2)	1.393 (4)
O1	0.4518 (3)	0.1685 (1)	0.6201 (2)	1.87 (4)
O5	0.0268 (3)	0.3689 (1)	0.8642 (2)	2.29 (4)
O11	−0.2002 (3)	0.4695 (2)	0.7155 (2)	3.55 (5)
O12	0.1679 (3)	0.4486 (2)	0.4855 (2)	3.15 (5)
O13	−0.2024 (3)	0.2417 (2)	0.5363 (2)	3.46 (5)
O21	0.3750 (3)	0.4420 (2)	0.9371 (2)	3.11 (5)
O22	0.6442 (3)	0.2405 (2)	0.7911 (2)	3.67 (6)
O23	0.4744 (4)	0.4695 (2)	0.6200 (2)	3.79 (6)
O31	−0.0550 (4)	0.1816 (2)	0.9467 (2)	3.43 (5)
O32	−0.0891 (3)	0.0757 (2)	0.6620 (2)	2.92 (5)
O33	0.3916 (4)	0.0881 (2)	0.8368 (2)	3.85 (6)
C1	0.2453 (4)	0.2630 (2)	0.6456 (2)	1.53 (5)
C2	0.3030 (4)	0.1938 (2)	0.5975 (2)	1.47 (5)
C3	0.2183 (4)	0.1510 (2)	0.5173 (2)	1.86 (5)
C4	0.5029 (4)	0.0858 (2)	0.5931 (2)	2.39 (6)
C5	0.0912 (4)	0.3375 (2)	0.7999 (2)	1.84 (5)
C11	−0.1109 (4)	0.4230 (2)	0.6883 (2)	2.29 (6)
C12	0.1227 (4)	0.4094 (2)	0.5460 (2)	2.16 (5)
C13	−0.1081 (4)	0.2771 (2)	0.5782 (2)	2.07 (5)
C21	0.3638 (4)	0.4052 (2)	0.8681 (2)	2.13 (5)
C22	0.5292 (4)	0.2750 (2)	0.7770 (2)	2.28 (6)
C23	0.4257 (4)	0.4215 (2)	0.6703 (2)	2.40 (6)
C31	0.0109 (4)	0.1895 (2)	0.8783 (2)	2.17 (5)
C32	−0.0107 (4)	0.1236 (2)	0.6987 (2)	1.97 (5)
C33	0.2946 (4)	0.1310 (2)	0.8109 (2)	2.34 (6)
H31	0.1152	0.1746	0.5090	
H32	0.2769	0.1581	0.4609	
H33	0.2087	0.0927	0.5308	
H41	0.6097	0.0772	0.6138	
H42	0.4361	0.0450	0.6214	
H43	0.4962	0.0804	0.5261	

[a] Parameters with an asterisk were refined isotropically. Anisotropically refined atoms are given in the form of the isotropic equivalent thermal parameter defined as $(^4/_3)$ $[a_2B(1,1) + b_2B(2,2) + c_2B(3,3) + ab(\cos\gamma)B(1,2) + ac(\cos\beta)B(1,3) + bc(\cos\alpha)B(2,3)]$.

Table IV. Bond Distances and Bond Angles (deg) for $Ru_3(CO)_{10}(\mu_3$-CC(OMe)Me) (**5**)[a]

atom 1	atom 2	distance	atom 1	atom 2	distance
Ru1	Ru2	2.793 (1)	Ru3	C31	1.932 (2)
Ru1	Ru3	2.777 (1)	Ru3	C32	1.934 (3)
Ru1	C1	2.056 (2)	Ru3	C33	1.930 (3)
Ru1	C5	2.154 (3)	O1	C2	1.346 (3)
Ru1	C11	1.972 (2)	O1	C4	1.439 (3)
Ru1	C12	1.940 (2)	O5	C5	1.176 (3)
Ru1	C13	1.921 (3)	O11	C11	1.126 (3)
Ru2	Ru3	2.773 (1)	O12	C12	1.130 (3)
Ru2	C1	2.066 (2)	O13	C13	1.132 (3)
Ru2	C5	2.158 (2)	O21	C21	1.140 (3)
Ru2	C21	1.954 (3)	O22	C22	1.126 (3)
Ru2	C22	1.950 (3)	O23	C23	1.125 (3)
Ru2	C23	1.931 (3)	O31	C31	1.127 (3)
Ru3	C1	2.161 (2)	O32	C32	1.128 (3)
Ru3	C2	2.782 (2)	O33	C33	1.120 (3)
Ru3	C5	2.226 (2)	C1	C2	1.387 (3)
			C2	C3	1.493 (3)

atom 1	atom 2	atom 3	angle	atom 1	atom 2	atom 3	angle
Ru2	Ru1	Ru3	59.73 (1)	Ru2	Ru1	C1	47.50 (8)
Ru2	Ru1	C5	49.68 (7)	Ru3	Ru1	C1	50.46 (8)
Ru3	Ru1	C5	51.81 (6)	C1	Ru1	C5	83.86 (8)
Ru1	Ru2	Ru3	59.84 (1)	Ru1	Ru2	C1	47.19 (8)
Ru1	Ru2	C5	49.58 (6)	Ru3	Ru2	C1	50.48 (8)
Ru3	Ru2	C5	51.85 (7)	Ru1	Ru3	Ru2	60.43 (2)
Ru1	Ru3	C1	47.21 (6)	Ru1	Ru3	C5	49.53 (8)
Ru2	Ru3	C1	47.54 (6)	Ru2	Ru3	C5	49.67 (8)
C2	O1	C4	119.4 (2)	Ru1	C1	Ru2	85.31 (8)
Ru1	C1	Ru3	82.33 (8)	Ru1	C1	C2	140.5 (2)
Ru2	C1	Ru3	81.98 (8)	Ru2	C1	C2	134.2 (2)
Ru3	C1	C2	101.0 (2)	O1	C2	C1	116.9 (2)
O1	C2	C3	118.2 (2)	C1	C2	C3	124.6 (2)
Ru1	C5	Ru5	80.74 (7)	Ru1	C5	Ru3	78.66 (8)
Ru1	C5	O5	133.1 (2)	Ru2	C5	Ru5	78.48 (8)
Ru1	C11	O11	176.4 (2)	Ru3	C5	O5	131.1 (2)
Ru1	C13	O13	178.6 (2)	Ru1	C12	O12	178.5 (2)
Ru2	C22	O22	177.9 (3)	Ru2	C21	O21	176.7 (2)
Ru3	C31	O31	178.9 (3)	Ru2	C23	O23	177.5 (2)
Ru3	C33	O33	178.3 (3)	Ru3	C32	O32	178.4 (2)

[a] Numbers in parentheses are estimated standard deviations in the least significant digits.

than the predicted angle of 120° for an idealized sp^2 hybrid. The C_α–C_β bond distance of 1.387 (3) Å is typical for a cluster-bound vinylidene ligand.[22] The least-squares plane containing the Ru_2C=C(OMe)Me vinylidene fragment makes an angle of 63° with the plane of the metals, resulting in a pronounced tilt of the vinylidene toward Ru3. The C1–Ru3 vector is significantly longer than the other two C1–metal vectors by about 0.1 Å, and the β-carbon C2 is outside bonding distance of Ru3 (2.782 (2) Å). Therefore it may be misleading to formulate the vinylidene as a σ,π-bound ligand. In the generally held view of σ,π-bound vinylidenes, the α-carbon is thought of as bridging one metal–metal vector through σ-bonds while the carbon–carbon double bond participates in π-bonding to the third metal.[23] The α-carbon is then within bonding distance of all three metals and the β-carbon within bonding distance of one of them. Such a formulation is supported by the few crystal structures which have been performed on capping vinylidenes.[22,23] As already mentioned, cluster **5** diverges from this configuration somewhat in that the β-carbon C2 is not within bonding distance of the metal framework (Figure 4). Therefore, this ligand may be viewed as intermediate between a σ,π-type capping ligand and a σ-bound bridging vinylidene. For purposes of electron counting the μ_3-C=C(OMe)Me ligand is counted as a four-electron donor. The C1–Ru3 vector is 0.1 Å longer than the other two metal–C1 bonds. Cleavage of the C1–Ru3 bond would convert the ligand into a μ-vinylidene and would result in the conversion of the molecule into an unsaturated 46-electron cluster. The facility with which cluster **5** exchanges H_2 for CO suggests that the 46-electron coordinately unsaturated isomer may be readily accessible.

^{13}C NMR Spectroscopy. The ^{13}C NMR shifts and carbon–carbon coupling constants provide unambiguous assignment of the ligand conformation and connectivity for many of the ruthenium clusters described here. The selective enrichment of CCO with ^{13}C was essential for the NMR studies. The α-carbon of the CCO is derived from a carbonyl ligand of $[Ru_3(CO)_{11}]^{2-}$ through activation followed by reductive cleavage.[2] As a result, the product contains ^{13}C at all carbons of the cluster, including the α-carbon of CCO, if the starting material $[Ru_3(CO)_{11}]^{2-}$ is ^{13}C-enriched. Furthermore, selective enrichment of the α-carbon of the CCO can be achieved by stirring enriched $[Ru_3(*CO)_{10}(*COC(O)CH_3)]^-$ under ^{12}CO, thus depleting ^{13}C in the terminal carbonyls while leaving ^{13}C in the $*COC(O)CH_3$ ligand. Reductive cleavage then generates $[Ru_3(CO)_9(\mu_3$-$*CCO)]^{2-}$ (**1**) which is exclusively enriched at the α-carbon. This procedure

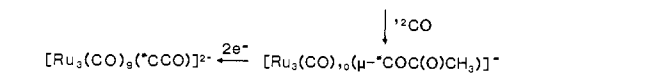

provides selectivively labeled compounds that can be used for the unambiguous assignment of the α-carbon resonance of all the products derived from **1**. Hence the fate of the α-carbon atoms were traced by ^{13}C NMR through the entire sequence of Scheme III.

The ^{13}C NMR resonances of the α- and β-carbons of the vinylidenes **5** and **6** appear between 140 and 220 ppm. This is also the chemical shift region in which many σ- and π-bonded ligands

(22) Bruce, M. I.; Swincer, A. G. *Adv. Organomet. Chem.* **1983**, *22*, 59.
(23) (a) Raithby, P. R.; Rosales, M. J. *Adv. Inorg. Chem. Radiochem.* **1986**, *29*, 169. (b) Roland, E.; Bernhardt, W.; Vahrenkamp, H. *Chem. Ber.* **1985**, *118*, 2858.

resonate,[23,24] and so the ^{13}C shifts are not indicative of the bonding mode. An apparently more reliable indication of conformation in these clusters is the magnitude of the ^{13}C–^{13}C coupling constant between the α- and β-carbon of the associated ligand. It has been established that $^1J_{CC}$ for the μ_4-η^2-bonded acetylene complex $Co_4(CO)_{10}(HC{\equiv}CH)$ is much smaller than that observed in free acetylene (21 vs. 171.5 Hz).[25] This drastic decrease, which has also been observed in the μ_3-η^2 complexes $Cp_2W_2Os(CO)_7(\mu_3$-η^2-$C_2Tol_2)$[26] and $Fe_3(CO)_9(\mu_3$-η^2-$HCC(O_2CCH_3))$,[17] is attributed to the extensive rehybridization which occurs on complexation of the acetylene ligand to the metal cluster. As already mentioned, the capping vinylidene ligand in **3** has a less pronounced interaction with the metal framework than a typical μ_3-η^2-acetylene. The $^1J_{CC}$ values for the (type A) compounds **5** and **6** are both in the range of 50 Hz, while those reported for the μ_3-η^2 and μ_4-η^2 (type B) compounds are all less than 25 Hz. Therefore, larger coupling

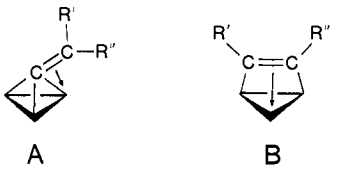

A B

constants are probably indicative of the upright μ_3 conformation of type A while the smaller $^1J_{CC}$'s imply a larger metal–ligand interaction as in the μ_3-η^2-bonding mode of type B. Hence it is possible to distinguish geometric isomers such as $H_2Ru_3(CO)_9(\mu_3$-CC(OMe)Me) (**6**) and $H_2Ru_3(CO)_9(\mu_3$-η^2-MeCCOMe)[27] on the basis of the $^1J_{CC}$ values.

The ^{13}C NMR assignments for the α- and β-carbons of all the compounds in this study were confirmed by selective enrichment experiments. As shown in Table I, the NMR signal of the α-carbon of the vinylidene **5** is upfield from the β-carbon. This order is reversed in compound **6**, in which the α-carbon appears downfield of the β-carbon. Apparently the vinylidene ligand in **6** is bound to the cluster in the conventional σ,π fashion, with the β-carbon within bonding distance of one of the metal vertices. The formulation is consistent with the observation that $^1J_{CC}$ for **6** is 5 Hz lower than that observed for the almost upright vinylidene **5**, indicating a stronger interaction with the metal framework.

In the alkylation reaction which forms complex **4** from **1** (Scheme I), the C_α–C_β coupling constant is observed to decrease from 96 Hz in $[Ru_3(CO)_9(\mu_3$-CCO)$]^{2-}$ to 44 Hz in $[Ru_3(CO)_{10}(\mu_3$-CC(O)$CH_3)]^-$. This is consistent with the view that the bond order between these two carbons decreases from a formal double bond in **1** to a single bond in **4**. Compound **4** is analogous to the previously characterized $Co_3(CO)_9(\mu_3$-CC(O)$CH_3)$.[28] The reaction of **1** with 25% ^{13}C-enriched CH_3I further establishes the connectivity of the capping ligand of **4**. In this case the methyl group is found to be coupled to both the α- and the β-carbons, with $^1J_{CC}$ = 42 Hz (to the β-carbon), and $^2J_{CC}$ = 20 Hz (to the α-carbon). This is comparable to the coupling observed in acetone, in which $^1J_{CC}$ = 40.1 Hz and $^2J_{CC}$ = 16 Hz.[29] The ^{13}C NMR shift of the α-carbon in **4** is at 191.8 ppm. The chemical shift region usually associated with capping alkylidyne ligands is from 250 to 350 ppm,[2,30] and so the apical carbon resonance of **4** appears anomalously far upfield.

In summary, the reactivity of the series of ketenylidene clusters $[Ru_3(CO)_9(\mu_3$-CCO$)]^{2-}$ (**1**), $[HRu_3(CO)_9(\mu_3$-CCO$)]^-$ (**2**), and $H_2Ru_3(CO)_9(\mu_3$-CCO) (**3**) was investigated. The monoanionic or neutral ketenylidenes $[HRu_3(CO)_9(\mu_3$-CCO$)]^-$ (**2**) and $H_2Ru_3(CO)_9(\mu_3$-CCO) (**3**) react with the nucleophile $LiCH_3$ to generate a cluster-bound acetyl moiety, while the doubly negative ketenylidene $[Ru_3(CO)_9(\mu_3$-CCO$)]^{2-}$ (**1**) reacts with the electrophile CH_3I to generate a similar cluster-bound acetyl. Although the products of the electrophilic and nucleophilic additions are similar, the routes that lead to their formation are apparently quite different. The reaction of CH_3I with $[Ru_3(CO)_9(\mu_3$-CCO$)]^{2-}$ (**1**) occurs through initial attack at the metals, followed by CO insertion and finally migration of the acetyl to the CCO ligand. By contrast, the nucleophilic reagent $LiCH_3$ appears to attack the β-carbon of the CCO ligand of $[HRu_3(CO)_9(\mu_3$-CCO$)]^-$ (**2**) or $H_2Ru_3(CO)_9(\mu_3$-CCO) (**3**) directly. Extended Hückel calculations suggest that for all three cases the addition reactions are orbital-controlled. The vinylidene $Ru_3(CO)_{10}(\mu_3$-CC(OMe)Me) (**5**) can be synthesized from the acetyl product $[Ru_3(CO)_{10}(\mu_3$-CC(O)Me$)]^-$ (**4**) via attack at the acyl oxygen atom by $CH_3OSO_2CF_3$. Dihydrogen readily substitutes for CO in the vinylidene cluster **5** to produce the dihydride $H_2Ru_3(CO)_9(\mu_3$-CC(OMe)Me) (**6**). This vinylidene dihydride can also be synthesized from $H_2Ru_3(CO)_9(\mu_3$-CCO) (**3**) by consecutive reaction with $LiCH_3$ and $CH_3OSO_2CF_3$. Thus depending on the starting material, either the electrophilic reagent CH_3I or the nucleophilic $LiCH_3$ can be used to generate **6**. The possibility of synthesizing the vinylidene $H_2Ru_3(CO)_9(\mu_3$-CC(OMe)Me) (**6**) from either $[Ru_3(CO)_9(\mu_3$-CCO$)]^{2-}$ *or* $H_2Ru_3(CO)_9(\mu_3$-CCO) is therefore not a reflection of the similar chemistry of these two compounds but rather the tendency for the metal cluster to stabilize the vinylidene ligand.

Acknowledgment. This research was supported by the NSF synthetic inorganic/organometallic chemistry program. M.J.S. is grateful for support from an ARCO fellowship.

Registry No. **1**, 97150-45-3; **2**, 110015-16-2; **3**, 90990-76-4; **4**, 110015-18-4; **5**, 110015-23-1; **6**, 110015-24-2; **7**, 110015-25-3; **9**, 110015-26-4; $Ru_3(CO)_{12}$, 15243-33-1; PPN^+Cl^-, 21050-13-5; $[PPN]_2[Ru_3(CO)_{11}]$, 97150-52-2; $[PPN]_2[Ru_3(*CO)_9(\mu_3$-*C*CO)], 110015-13-9; $[PPN]_2[Ru_3(CO)_9$*CCO], 109527-95-9; $[PPN]_2[Ru_3(CO)_9$*C*CO], 110015-15-1; $[PPN][Ru_3(CO)_{10}(\mu_3$-*C*C(O)$CH_3)]$, 110015-20-8; $[PPN][Ru_3(*CO)_{10}(\mu_3$-*C*C(O)$CH_3)]$, 110015-22-0.

Supplementary Material Available: A table of values of refined anisotropic thermal parameters for **5** (2 pages); a listing of F_o and F_c for **5** (47 pages). Ordering information is given on any current masthead page.

(24) Aime, S.; Milone, L.; Osella, D.; Valle, M.; Randall, E. W. *Inorg. Chim. Acta* **1976**, *20*, 217.
(25) Aime, S.; Osella, D.; Giamello, E.; Granozzi, G.; *J. Organomet. Chem.* **1984**, *262*, C1.
(26) Chi, Y.; Shapley, J. R. *Organometallics* **1985**, *4*, 1900.
(27) Churchill, M. R.; Fettinger, J. C.; Keister, J. B.; See, R. F.; Ziller, J. W. *Organometallics* **1985**, *4*, 2112.
(28) ^1H NMR ($CDCl_3$) 2.60 ppm (s, CH_3); IR $\nu_{C=O}$ 1640 (s) cm^{-1}. For **4**: ^1H NMR (CD_2Cl_2) 2.34 ppm (s, CH_3); IR $\nu_{C=O}$ 1590 (m) cm^{-1}): Seyferth, D.; Hallgren, J. E.; Hung, P. L. K. *J. Organomet. Chem.* **1973**, *50*, 265.
(29) Abraham, R. J.; Loftus, P. *Proton and Carbon-13 NMR Spectroscopy*; Heyden and Son: London, 1980.
(30) Aime, S.; Milone, L.; Valle, M. *Inorg. Chim. Acta* **1976**, *18*, 9.